

# A Three-Phase Active Power Filter Operating with Fixed Switching Frequency for Reactive Power and Current Harmonic Compensation

Luis A. Morán, *Member, IEEE*, Juan W. Dixon, *Member, IEEE*, and Rogel R. Wallace

**Abstract**—The performance and dynamic characteristics of a three-phase active power filter operating with fixed switching frequency is presented and analyzed in this paper. The proposed scheme employs a PWM voltage-source inverter and has two important characteristics. First, it operates with fixed switching frequency, and second, it can compensate the reactive power and the current harmonic components of nonlinear loads. Reactive power compensation is achieved without sensing and computing the reactive component of the load current, thus simplifying the control system. Current harmonic compensation is done in time domain.

The principles of operation of the proposed active power filter along with the design criteria of the power and control circuit components are discussed in detail. Finally, experimental results obtained from a 5-kVA prototype confirm the feasibility and the features of the proposed system.

## I. INTRODUCTION

THE proliferation of nonlinear loads such as static power converters and arc furnaces results in a variety of undesirable phenomena in the operation of power systems. The most important among these are harmonic contamination, increased reactive power demand and power system voltage fluctuations. Harmonic contamination has become a major concern for power system specialists due to its effects on sensitive loads and on the power distribution system. Harmonic current components increase power system losses, cause excessive heating in rotating machinery, can create significant interference with communication circuits that shared common right-of-ways with ac power lines, and can generate noise on regulating and control circuits causing erroneous operation of such equipment.

Conventionally, passive LC filters have been used to eliminate line current harmonics and to increase the load power factor. However, in practical applications these passive second order filters present the following disadvantages:

- 1) The source impedance strongly affects filtering characteristics.
- 2) As both the harmonic and the fundamental current components flow into the filter, the capacity of the filter must be rated by taking into account both currents.
- 3) When the harmonic current components increase, the filter can be overloaded.
- 4) Parallel resonance between the power system and the passive filter causes amplification of harmonic currents on the source side at a specific frequency.
- 5) The passive filter may fall into series resonance with the power system, so that voltage distortion produces excessive harmonic currents flowing into the passive filter.

In order to overcome these problems, active power filters have been researched and developed [1]. In recent years, various active power filter configurations with their respective control strategies have been proposed, and have gradually been recognized as a viable solution to the problems created by high-power nonlinear loads [2]–[6].

The topology of the three-phase active power filter presented in this paper is shown in Fig. 1. The proposed configuration is based on a force-commutated pulse-width modulated voltage-source inverter (PWM-VSI) connected to a dc capacitor. Although there are a number of articles which deal with the analysis of active power filters using force-commutated voltage-source inverters [1], [4]–[6], the three-phase active power filters presented in this paper differs from previously discussed approaches in the following ways:

- 1) Reactive power compensation is achieved without sensing and computing the reactive current component of the load, thus simplifying the control circuit.
- 2) Current control is achieved with constant switching frequency producing a better switching pattern than hysteresis current control [7]. This results in a reduction of inverter output high-frequency current harmonics and lower stresses on the semiconductor devices.
- 3) Current compensation is done in time domain allowing fast time response.
- 4) In order to improve the active power filter performance, a dc voltage control loop is implemented. The dc voltage control loop keeps the voltage across the dc capacitor constant, increasing the inverter voltage gain and

Manuscript received June 6, 1995; revised July 27, 1994 and March 31, 1994. This work received support from the Fondo de Desarrollo Científico y Tecnológico "FONDECYT" through the 92-0262 Project and the Dirección de Investigación of the University of Concepción, the International Copper Association, and the Agency of International Development through Project no. 20.92.11, I.C.A. no. 416, and A.I.D. no. 11.196.

L. Morán and R. Wallace are with the Department of Electrical Engineering, University of Concepción, Concepción, Chile.

J. W. Dixon is with the Department of Electrical Engineering, Universidad Católica de Chile, Santiago, Chile.

IEEE Log Number 9412493.

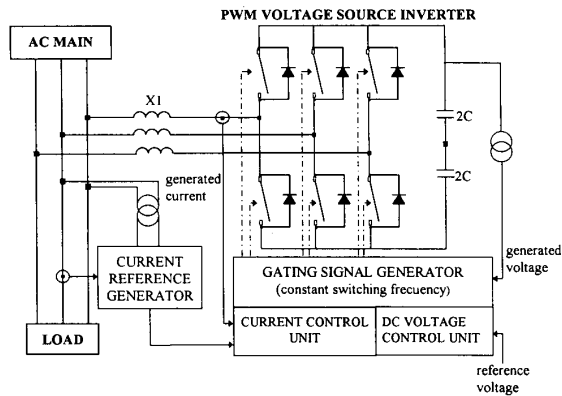


Fig. 1. The active power filter configuration.

reducing the amplitude of high-frequency ac current harmonics.

- 5) The voltage and current control loops are simple and easy to implement.

Moreover, compared to series active power filters [11], the active power filter presented in this paper is connected in parallel with the load, thus compensating current waveform and not voltage as in series active filters. Also, shunt active power filters are easy to protect against power system short circuit currents. By using a fixed switching frequency, the high-frequency ripple current generated by the proposed active power filter can be easily removed from the power system.

The treatment presented in this paper includes a comprehensive steady-state and transient analysis of the active power filter. Also, the design criteria of the power and the control circuit are reported. Finally, all the predicted results are experimentally verified on a 5-kVA laboratory prototype.

## II. PRINCIPLES OF OPERATION

The main section of the active power filter shown in Fig. 1 is a force-commutated voltage-source inverter connected to a dc capacitor. Current harmonic compensation is achieved by injecting equal but opposite current harmonic components at the point of connection, thereby canceling the original distortion and improving the power quality on the connected power system [2], [3].

The block diagram of the active filter control system is shown in Fig. 2. It consists of a current control unit, a dc voltage control unit, a current reference generator, and a gating signals generator.

The ac current generated by the inverter is forced to follow the reference signal obtained from the current reference generator. In this circuit, the distorted load current is filtered extracting the fundamental component,  $i_{l1}$ . The band-pass filter is tuned at the fundamental frequency (50 or 60 Hz), so that the gain attenuation introduced in the filter output signal is zero and the phase shift angle is  $180^\circ$ . Thus, the filter output current is exactly equal to the fundamental component of the load current but phase shifted by  $180^\circ$ . If the load current is added to the fundamental current component obtained from the second order band-pass filter, the reference current waveform

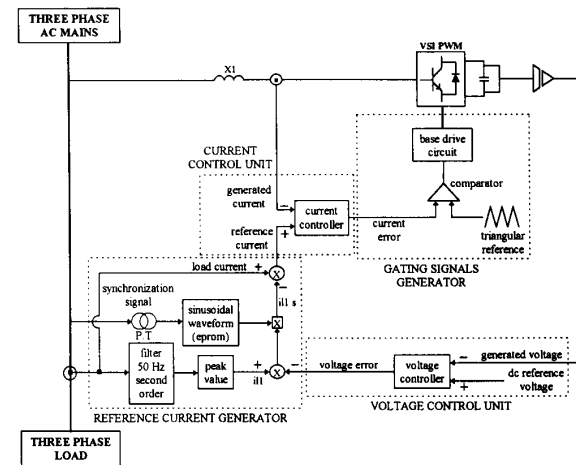


Fig. 2. Block diagram of the active power filter control system.

required to compensate only harmonic distortion is obtained. In order to provide the reactive power required by the load, the current signal obtained from the second order band-pass filter,  $I_{l1}$ , is synchronized with the respective phase-to-neutral source voltage (see Fig. 3), so that the inverter ac output current is forced to lead the respective inverter output voltage, thereby generating the required reactive power and absorbing the real power necessary to maintain the dc voltage constant and to supply the switching losses. The real power absorbed by the inverter is controlled by adjusting the amplitude of the fundamental current reference waveform,  $I_{l1}$ , obtained from the reference current generator (see Fig. 2). The amplitude of this sinusoidal waveform is equal to the amplitude of the fundamental component of the load current plus or minus the error signal obtained from the dc voltage control unit. In this way, the current signal allows the inverter to supply the current harmonic components, the reactive power required by the load, and to absorb the small amount of active power necessary to cover the switching losses and to keep the dc voltage constant. By keeping the dc voltage constant, the inverter voltage gain is increased and the amplitude of the high-frequency inverter current harmonic component is reduced.

A constant switching frequency is achieved by comparing the current error signal with a triangular reference waveform. This method can be explained by considering the bang-bang hysteresis technique plus the addition of a fixed frequency triangular waveform inside the imaginary hysteresis window [8]. The purpose of introducing the triangular waveform is to stabilize the converter switching frequency by forcing it to be constant and equal to the frequency of the triangular reference signal. Since the current error signal is always kept within the negative and positive peaks of the triangular waveform (see Fig. 2), the system has an inherent overcurrent protection. A large variation in the reference current will generate a large error signal which can be higher than the amplitude of the triangular waveform. In this case, there will not be an intersection between the error and the triangular waveform,

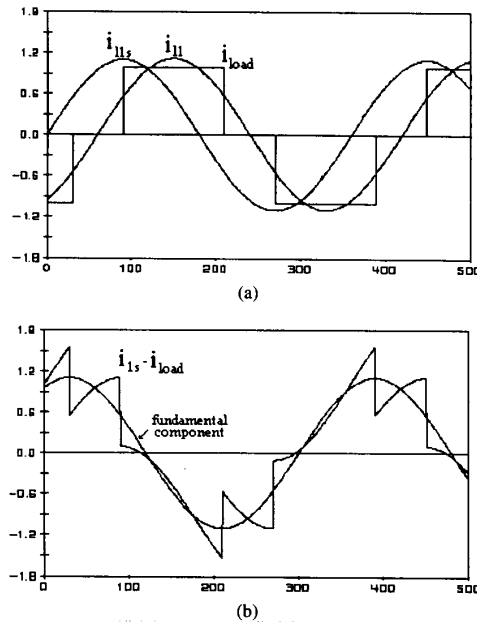


Fig. 3. The procedure for the generation of the current reference waveform. (a) The load current,  $i_{load}$ , its fundamental component,  $i_{l1}$ , and the fundamental current component synchronized with the respective phase-to-neutral source voltage,  $i_{l1s}$ . (b) The synchronized fundamental current signal minus the load current,  $i_{l1s} - i_{load}$ , and its fundamental component.

thus the switching pattern will not change until the current error signal is reduced and a new intersection occurs.

It is important to notice that the proposed control system is stable and independent of the power system characteristics. If the power system has a finite impedance, so that the source voltages present harmonic components or are unbalanced, the ripple voltage across the dc capacitor will increase, generating a higher THD at the inverter output voltages. This problem can be solved by increasing the capacitance value of the electrolytic capacitor [9].

The stability of the active power filter is reflected by its ability to keep the dc voltage close to the reference value. Previous work has demonstrated that the stability of active power filters implemented with self-controlled dc bus voltage-source inverters is independent of parameter values (synchronous link reactor and dc capacitor) [10]. In this case, the active power filter stability can be guaranteed by limiting the small amount of maximum real power absorbed by the inverter. This can be done by fixing the maximum value of the voltage error signal, thus limiting the amplitude of the fundamental component of the current reference waveform,  $I_{l1}$ .

A nonideal band-pass filter will affect the generation of the reference current, specifically the detection of the fundamental component peak value of the load current and the phase-shift angle between the current  $i_{l1s} - i_{load}$  and the respective phase-to-neutral voltage (see Fig. 3). This will modify the amount of real and reactive power generated by the active power filter, affecting the ac source power factor value, and the inverter dc

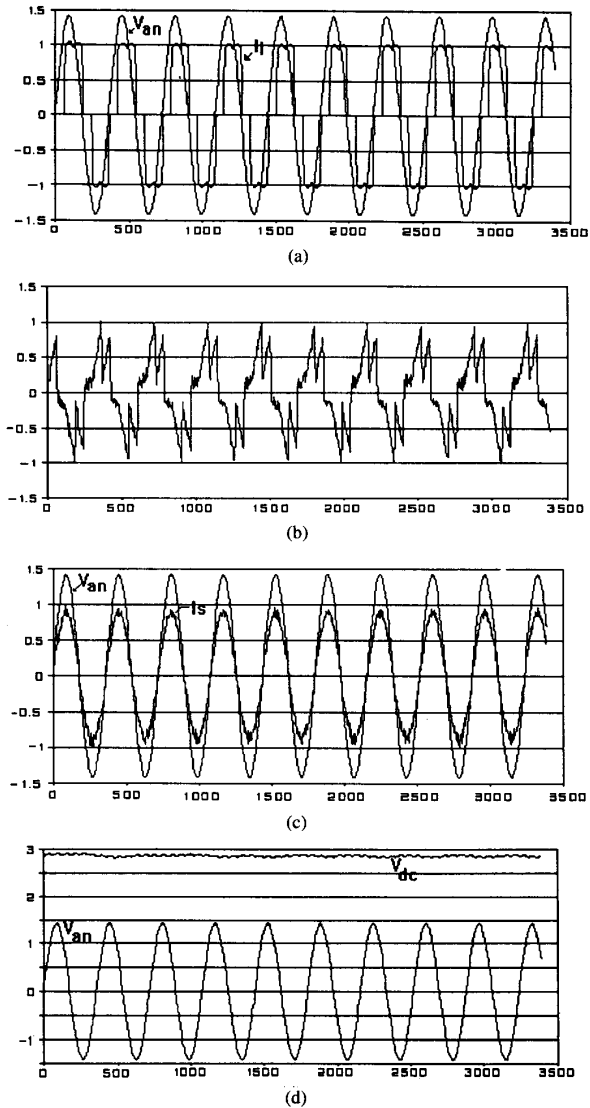


Fig. 4. Simulated results for steady state operating conditions. (a) Phase-to-neutral source voltage,  $V_{an}$ , and respective load current,  $I_l$ . (b) Inverter ac output current. (c) phase-to-neutral source voltage,  $V_{an}$ , and the respective ac mains line current,  $I_s$ . (d) The voltage across the dc capacitor,  $V_{dc}$ , and the phase-to-neutral ac mains voltage,  $V_{an}$ .

voltage. However, the inverter dc voltage is forced to remain closed to the reference value by the closed loop control.

Figs. 4 and 5 show simulated current and voltage waveforms for steady state and transient operating conditions. In both cases the active power filter is compensating a six step controlled rectifier. Fig. 4 proves that the active power filter compensates harmonic component and the reactive power effectively. Also, this figure illustrates how the inverter gain voltage is improved with the addition of the dc voltage control loop [Gain = 0.85 (see Fig. 4(d))].

In Fig. 5, a step change in the load power factor and current amplitude is simulated. The amplitude of the load current is

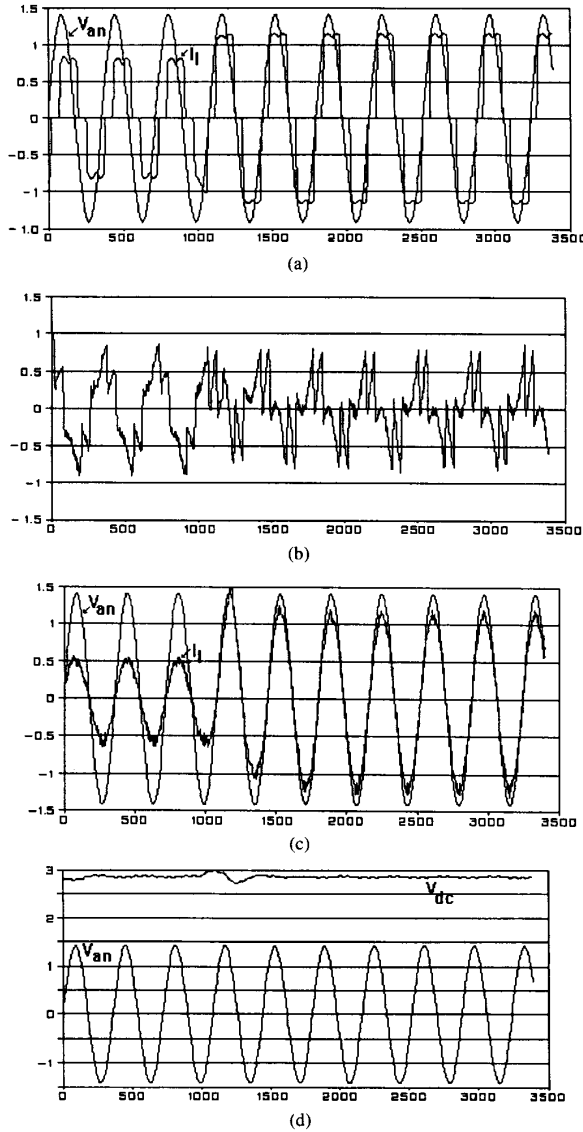


Fig. 5. Simulated results for transient operating conditions. (a) The phase-to-neutral source voltage,  $V_{an}$ , and the respective load current,  $I_l$ . (b) Inverter ac output current. (c) Phase-to-neutral source voltage,  $V_{an}$ , and the respective ac mains line current,  $I_s$ . (d) The voltage across the dc capacitor,  $V_{dc}$ , and the phase-to-neutral source voltage,  $V_{an}$ .

changed from 0.4–0.8 in p.u. while the phase shift angle,  $\alpha$ , decreases from  $45^\circ$ – $15^\circ$ . These figures show that the active power filter is fast enough to respond to this severe change in the load operating condition, keeping the source line current in phase with the respective phase-to-neutral voltage and with a low harmonic distortion.

### III. POWER CIRCUIT DESIGN

The selection of the ac link reactor and the dc capacitor values affects directly the performance of the active power filter. Static var compensators implemented with voltage-

source inverters present the same power circuit topology, but for this type of application, the criteria used to select the values of  $L$  and  $C$  are different. For reactive power compensation, the design of the synchronous link inductor,  $L$ , and the dc capacitor,  $C$ , is performed based on harmonic distortion constraint. That is,  $L$  must reduce the amplitude of the current harmonics generated by the inverter while  $C$  must keep the dc voltage ripple factor below a given value [9]. This design criteria cannot be applied in the active power filter since it must be able to generate distorted current waveforms. However,  $L$  must be specified so that it keeps the high-frequency ripple of the inverter ac output current smaller than a defined value.

#### A. Design of the Synchronous Link Reactor

The design of the synchronous link reactor is performed with the constraint that for a given switching frequency the minimum slope of the inductor current is smaller than the slope of the triangular waveform that defines the switching frequency (see Fig. 2). In this way, the intersection between the current error signal and the triangular waveform will always exist.

The slope of the triangular waveform,  $\lambda$ , is defined by

$$\lambda = 4\xi f_t \quad (1)$$

where  $\xi$  is the amplitude of the triangular waveform, which has to be equal to the maximum permitted amount of ripple current, and  $f_t$  is the frequency of the triangular waveform (i.e., the inverter switching frequency). The maximum slope of the inductor current is equal to

$$\frac{di_L}{dt} = \frac{V_{an} + 0.5 V_{dc}}{L} \quad (2)$$

Since the slope of the inductor current has to be smaller than the slope of the triangular waveform, and the ripple current is known, from (1) and (2)

$$L = \frac{V_{an} + 0.5 V_{dc}}{4\xi f_t} \quad (3)$$

#### B. Design of the DC Capacitor

Transient changes in the instantaneous power absorbed by the load generate voltage fluctuations across the dc capacitor (see Fig. 5(d)). The amplitude of these voltage fluctuations can be controlled effectively with an appropriate dc capacitor value. It must be noticed that the dc voltage control loop stabilizes the capacitor voltage after a few cycles, but is not fast enough to limit the first voltage variations. The capacitor value obtained with this criteria is bigger than the value obtained based on maximum dc voltage ripple constraint. For this reason, the voltage across the dc capacitor presents a smaller harmonic distortion factor.

The maximum overvoltage generated across the dc capacitor is given by

$$V_{c\max} = \frac{1}{C} \int_{(\theta_1/\omega)}^{(\theta_2/\omega)} i_c(t) dt + V_{dc} \quad (4)$$

TABLE I  
DESIGN DATA FOR POWER CIRCUIT

Synchronous Link Reactor	$X_l = 0.12$ pu	$S = 0.12$ pu
Dc Capacitor	$X_c = 12$ pu	$S = 1.59$ pu

where  $V_{cmax}$  is the maximum voltage across the dc capacitor,  $V_{dc}$  is the steady-state dc voltage, and  $i_c(t)$  is the instantaneous dc bus current.

From (4)

$$C = \frac{1}{\Delta V} \int_{(\theta_1/\omega)}^{(\theta_2/\omega)} i_c(t) dt. \quad (5)$$

Equation (5) gives the value of the dc capacitor,  $C$ , that will maintain the dc voltage fluctuation below  $\Delta V$  p.u. The instantaneous value of the dc current is defined by the product of the inverter line currents with the respective switching functions. The mean value of the dc current that generates the maximum overvoltage can be estimated by

$$\int_{(\theta_1/\omega)}^{(\theta_2/\omega)} i_c(t) dt = I_{inv} \int_{(\theta_1/\omega)}^{(\theta_2/\omega)} [\sin(\omega t) + \sin(\omega t + 120^\circ)] dt. \quad (6)$$

In this expression the inverter ac current is assumed to be sinusoidal. These operating conditions represent the worst case. Table I summarizes the design data for the synchronous link reactor, the inverter power switches and the dc capacitor, in p.u. with respect to the ac phase-to-neutral base values. The design data presented in Table I are valid for an inverter switching frequency equal to 1.5 kHz, a modulation index of 0.7, and a THD of the ac source current of 5%.

Power switches must be rated with 0.5-p.u. current and 2.5-p.u. peak forward blocking voltage.

#### IV. CONTROL CIRCUIT DESIGN

The design procedure for the current and voltage loops is based on the respective time response requirements. Since the transient response of the active power filter is determined by the current control loop, its time response has to be fast enough to follow the current reference waveform closely. On the other hand, the time response of the dc voltage control loop does not need to be fast and is selected to be at least ten times slower than the current loop time response. Thus, these two control systems can be decoupled and designed as two independent systems.

A PI controller is selected for the current and the voltage control loops since it contributes to zero steady-state error in tracking the reference current and voltage signals, respectively.

##### A. Design of the Current Control Loop

Each PWM inverter current control loop consists of three independent PI controllers. Since the active power filter is im-

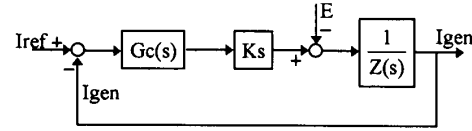
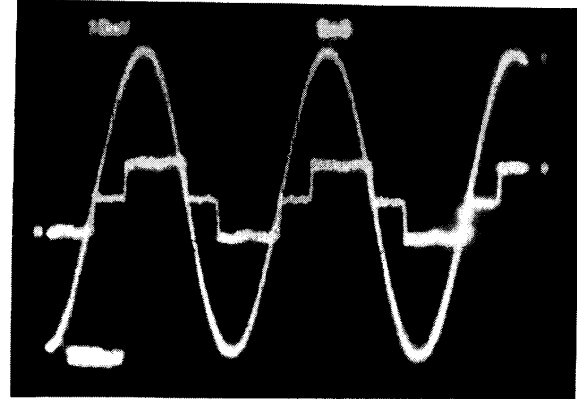
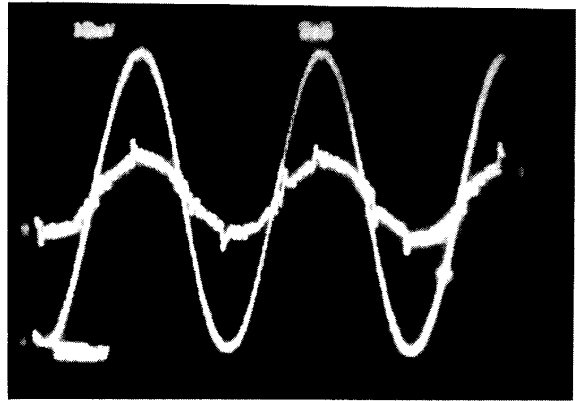


Fig. 6. The block diagram of the current control loop.



(a)



(b)

Fig. 7. Steady-state experimental results. (a) The phase-to-neutral source voltage,  $V_{an}$ , 50 V/div, and the respective load current, 5 A/div. (b) The phase-to-neutral source voltage,  $V_{an}$ , 50 V/div, and the respective source current, 5 A/div.

plemented with voltage-source inverters, the ac output current is defined by the inverter ac output voltage. The block diagram of the current control loop for each phase is shown in Fig. 6 where

- $E$  phase-to-neutral source voltage,
- $Z(s)$  impedance of the synchronous reactor,
- $X_l, K_s$  gain of the converter, and
- $G_c(s)$  gain of the PI controller.

The values of  $K_s$  and  $G_c(s)$  are given in (7) and (8).

$$K_s = \frac{V_{dc}}{2\xi} \quad (7)$$

$$G_c(s) = K_p + \frac{K_i}{s}. \quad (8)$$

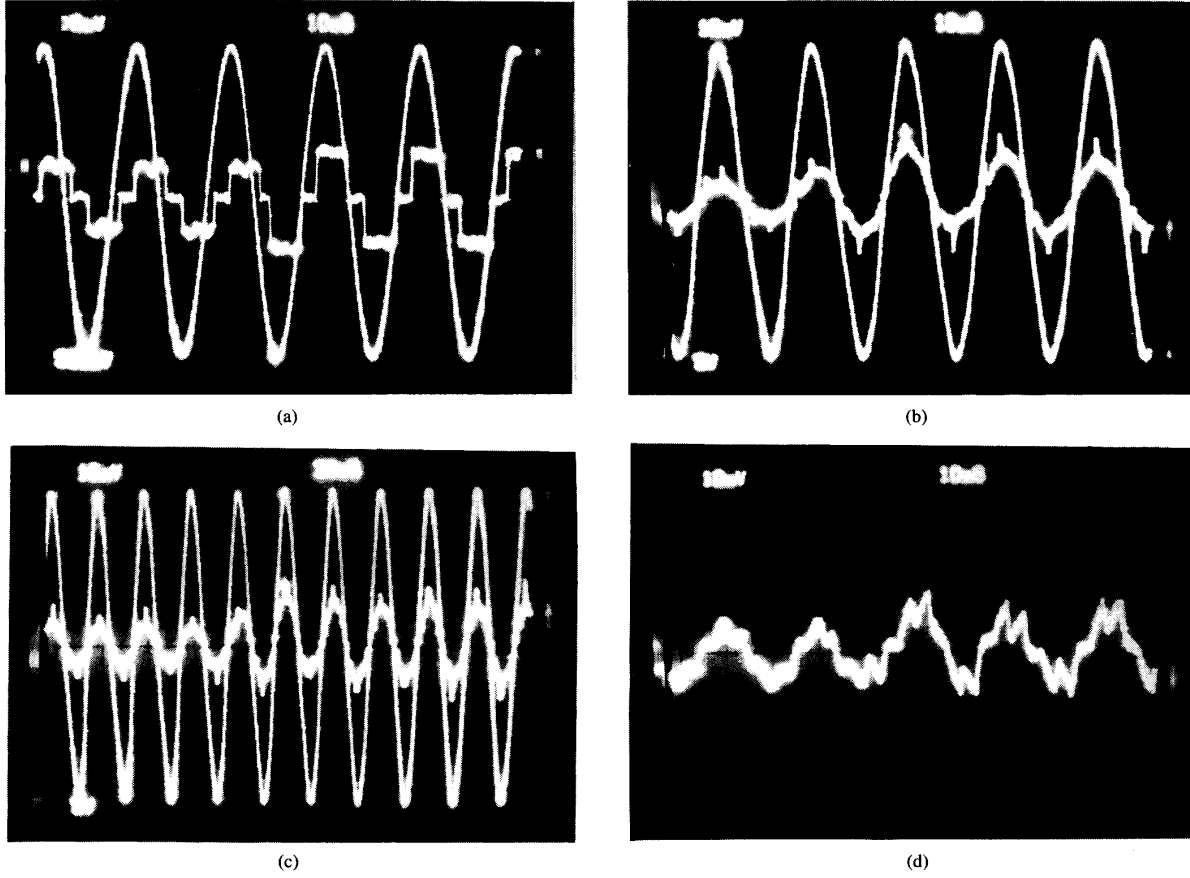


Fig. 8. Transient experimental results. (a) Phase-to-neutral voltage, 50 V/div, and load current, 5 A/div. (b) Phase-to-neutral voltage, 50 V/div, and the source line current, 5 A/div. (c) Phase-to-neutral source voltage, 50 V/div, and the source current, 5 A/div. (d) The inverter output current, 5 A/div.

From Fig. 6 and using (8), the following expression is obtained:

$$\mathbf{I}_{\text{gen}} = \frac{K_s \left( K_p + \frac{K_i}{s} \right)}{R_r + sL_r} \mathbf{I}_{\text{ref}} - \frac{1}{1 + \frac{K_s \left( K_p + \frac{K_i}{s} \right)}{R_r + sL_r}} \mathbf{E}. \quad (9)$$

The characteristic equation of the current control loop is given by

$$1 + \frac{K_p s + \frac{K_i}{s}}{s(R_r + sL_r)} = 0. \quad (10)$$

The analysis of the characteristic equation proves that the current control loop is stable for all values of  $K_p$  and  $K_i$ . Also, this analysis shows that  $K_p$  determines the speed response and

$K_i$  defines the damping factor of the control loop. If  $K_p$  is too big, the error signal can exceed the amplitude of the triangular waveform, affecting the inverter switching frequency, and if  $K_i$  is too small, the gain of the PI controller decreases, which means that the generated current will not be able to follow the reference current closely.

Simulated results have shown that the compensator transient response is improved by adjusting the gain of the proportional part ( $K_p$ ) to equal one and the gain of the integrator ( $K_i$ ) to equal the frequency of the triangular waveform.

#### B. DC Voltage Control Loop

In order to eliminate the steady-state error in the dc voltage, a PI controller is used. The proportional gain and the integral gain are equal to 4.8 and 2000 rad/s, respectively (ten times slower than the current control loop). More details concerning the design of this control loop are presented in [10].

## V. EXPERIMENTAL RESULTS

A 5-kVA laboratory prototype using IGBT switches was implemented and successfully tested in compensating a six-step controlled rectifier. The inverter was operated at a 1.5-KHz

switching frequency. Steady-state and transient results obtained with this breadboard unit are depicted in Figs. 7 and 8.

Steady-state experimental results for a nonlinear compensation are illustrated in Fig. 7. Fig. 7(a) shows the line-to-neutral ac mains voltage with the respective load current (three-phase controlled rectifier). In Fig. 7(b), the phase-to-neutral source voltage with the respective source line current is illustrated. This figure shows that the active power filter eliminates low frequency harmonic components effectively and is able to compensate the reactive power required by the load (phase shift angle is almost zero).

Transient results are shown in Fig. 8. A transient operating condition is obtained by generating a step change in the firing angle (from  $\alpha = 45^\circ$  to  $\alpha = 15^\circ$ ) of the three-phase controlled rectifier. In particular, Fig. 8(a) shows the transient step change in the load current and in the power factor. In Fig. 8(b), the ac mains phase-to-neutral source voltage with the respective line current is shown. This figure shows the effectiveness of the active power filter, since it is able to keep the current in phase with the respective phase-to-neutral voltage, thereby keeping the ac source power factor equal to one, and eliminating low-frequency current harmonics. Fig. 8(c) shows that the line current reaches steady-state in almost two cycles. This result proves that the time response of the current loop control is fast. Finally, Fig. 8(d) shows the respective inverter output current.

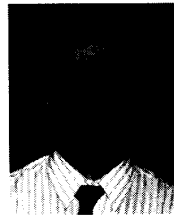
Comparison with simulated waveforms shown in Figs. 4 and 5 reveals a close agreement between predicted and experimental waveforms. Moreover, agreement in waveforms validates the analysis presented.

## VI. CONCLUSION

In this paper, an active power filter that operates with fixed switching frequency has been presented and analyzed. The proposed active power filter can compensate current harmonic components and the reactive power required by the load. Reactive power compensation is achieved without sensing and computing the associated reactive power component, thus simplifying the circuit topology. The performance of the active power filter has been improved by including a dc voltage control loop that maintains the voltage across the dc capacitor constant. In this way, the inverter voltage gain is increased and the high-frequency ripple current is reduced. The close agreement between the analytical and the experimental results proves the validity of the analysis and the feasibility of the proposed system.

## REFERENCES

- [1] W. M. Grady, M. J. Samotyj, and A. H. Noyola, "Survey of active power line conditioning methodologies," *Trans. Power Delivery*, vol. 5, no. 3, pp. 1536-1542, July 1990.
- [2] L. Gyugyi and E. C. Strycula, "Active ac power filters," in *Conf. Rec. IEEE Ind. Applicat. Soc. Annu. Meeting*, Oct. 1976, pp. 529-535.
- [3] H. Kawahira, T. Nakamura, S. Nakazawa, and M. Nomura, "Active power filter," in *Proc. JIEE IPEC*, Mar. 1983, pp. 981-992.
- [4] H. Akagi, Y. Kanazawa, and A. Nabae, "Instantaneous reactive power compensators comprising switching devices without energy storage components," *IEEE Trans. Ind. Applicat.*, vol. IA-20, no. 3, pp. 625-630, May/June 1984.
- [5] H. Akagi, A. Nabae, and S. Atoh, "Control strategy of active power filters using multiple voltage-source PWM converters," *IEEE Trans. Ind. Applicat.*, vol. IA-22, no. 3, pp. 460-465, May/June 1986.
- [6] L. Malesani, L. Rossetto, and P. Tenti, "Active filters for reactive power and harmonic compensation," in *Proc. IEEE PESC*, June 1986, pp. 321-330.
- [7] R. Wu, S. Dewan, and G. Slemon, "A PWM ac to dc converter with fixed switching frequency," *IEEE Trans. Ind. Applicat.*, vol. 26, no. 5, pp. 880-885, Sept./Oct. 1990.
- [8] M. Kazerani, P. D. Ziogas, and G. Joos, "A novel active current waveshaping technique for solid-state input power factor conditioners," *IEEE Trans. Ind. Electron.*, vol. 38, no. 1, pp. 72-78, Feb. 1991.
- [9] L. Morán, P. D. Ziogas, and G. Joós, "Analysis and design of a novel three-phase solid-state power factor compensator and harmonic suppressor system," *IEEE Trans. Ind. Applicat.*, vol. 25, no. 4, pp. 609-619, July/Aug. 1989.
- [10] ———, "Performance analysis of a PWM inverter var compensator," *IEEE Trans. Power Electron.*, vol. 6, no. 3, pp. 380-391, July 1991.
- [11] F. Z. Peng, H. Akagi, and A. Nabae, "A new approach to harmonic compensation in power systems," in *Conf. Rec. IEEE Ind. Applicat. Soc. Annu. Meeting*, 1988, pp. 874-880.



**Luis A. Morán** (S'78-M'82) was born in Concepción, Chile, in 1958. He received the electrical engineering degree from the University of Concepción in 1982, and the Ph.D. degree in electrical engineering from Concordia University, Montreal, Canada, in 1990.

Since 1990, he has been with the Department of Electrical Engineering, University of Concepción, where he is an Associate Professor. He is a consultant for several industrial projects. His research area is in var compensation, active power filters,

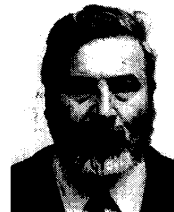
and power distribution systems.



**Juan W. Dixon** (M'90) was born in Santiago, Chile, in 1948. He received the electrical engineering degree from the University of Chile in 1977, and the M.Eng. and Ph.D. degrees in electrical engineering from McGill University, Montreal, Canada, in 1986 and 1988, respectively.

Since 1979, he has been an Associate Professor in the Department of Electrical Engineering, Catholic University of Chile, Santiago, teaching the subjects of power electronics and electrical machines. His research interests have included electric traction,

machine drives, frequency changers, high-power rectifiers, static var compensators, and active power filters.



**Rogel R. Wallace** was born in Santiago, Chile, in 1942. He received the electrical engineering degree from the Universidad Técnica Federico Santa María in 1966, the Ph.D. degree from the Moscow Power Institute, U.S.S.R. (now Russia), in 1976.

He was a postdoctoral fellow in electrical machine design at the Moscow Power Institute. Since 1980, he has been with the Department of Electrical Engineering, University of Concepción, Chile, where he is a Professor. His teaching activities and research interests include electrical machine design,

power electronics, variable frequency drives, and control system theory applied to electrical drives.